Composites Science and Technology 118 (2015) 276–283

Contents lists available at ScienceDirect

Composites Science and Technology

journal homepage: http://www.elsevier.com/locate/compscitech

A simplistic unit cell model for sound absorption of cellular foams with fully/semi-open cells

X.H. Yang [a, b], S.W. Ren [b, c], W.B. Wang [b], X. Liu [a], F.X. Xin [b, c], T.J. Lu [b, c, *]

[a] Department of Building Environment and Energy Engineering, Xi'an Jiaotong University, Xi'an 710049, China
[b] MOE Key Laboratory for Multifunctional Materials and Structures, Xi'an Jiaotong University, Xi'an 710049, China
[c] State Key Laboratory for Mechanical Structure Strength and Vibration, School of Aerospace, Xi'an Jiaotong University, Xi'an 710049, China

ARTICLE INFO

Article history:
Received 13 June 2015
Received in revised form
7 September 2015
Accepted 9 September 2015
Available online 11 September 2015

Keywords:
Fibres
Mechanical properties
Modelling
Acoustic emission

ABSTRACT

We present a simplistic yet accurate unit cell model of sound absorption for highly porous foams having either fully-open or semi-open cells. Employing an idealized periodic cubic unit cell to mimic the foam topology, we establish an analytical model for predicting the sound absorption coefficient of the foam. Analytical links between key non-acoustic parameters (viscous permeability and flow tortuosity) and cellular topological characteristics are also established. For fully-open foams, the model requires only two morphological parameters, porosity and pore window size, significantly reducing the complexity of sound transport modeling. For semi-open foams, an additional parameter, open-pore rate representing the influence of thin membrane covering on pore window, is introduced. The analytical model predictions are compared with existing experimental data and numerical simulation results for polyurethane foams, with good agreement achieved.

1. Introduction

High porosity open-cell foams have shown distinctive properties, along with relatively low manufacturing cost, ultra-low density and high surface area-to-volume ratio. They have been, therefore, utilized in a variety of engineering applications, especially in sound absorbers and vibration isolators [1]. To characterize sound propagation in such foams and other porous media, the sound absorption coefficient (SAC) is a key parameter. Knowledge of the SAC is also helpful for the optimization and design of noise control applications.

Studies on the SAC of open-cell foam-type porous media have been carried out numerically [2,3], experimentally [4–9] and analytically [10–14]. Directly determination of the SAC via experimental measurement is very important and can provide benchmark for validations of numerical or theoretical models. Numerical simulations on the sound propagation in porous materials have been recently developed and have attracted more and more attention due to their robustness in computing complex porous materials and visualization capability of sound propagation. In comparison, analytical models of SAC have clear superiority in revealing physical mechanisms if the models are built upon sound physical basis. Stemming from the 1940s, as shown in Fig. 1, the number of parameters needed for analytically predicting the SAC of various kinds of rigid porous media has increased from one to eight in order to obtain more accurate description of sound propagation and viscous-inertial/thermal energy dissipation in the tortuous porous path [15]. For instance, the Jonhson-Champoux-Allard-Pride-Lafarge model has been so far supposed to be the most accurate and complex analytical model, which requires eight parameters as input information.

Open-cell foams have stochastic, complex and tortuous microstructures. Predicting accurately the amount of sound absorbed by the foam requires precise estimates of key non-acoustic parameters such as viscous/thermal permeability, viscous/thermal characteristic length and tortuosity factor, as indicated by selected analytical models summarized in Fig. 1. Up to now, existing attempts to predict the SAC of open-cell foams have focused on determining key non-acoustic parameters via either unit cell (UC) reconstruction or numerical homogenization [16].

Perrot et al. [4] used an idealized tetrakaidecahedron unit cell to model the microstructure of open-cell foams and deduced macro properties from micro-structural features. Doutres et al. [6] measured the non-acoustic parameters of 15 polyurethane foams

* Corresponding author. MOE Key Laboratory for Multifunctional Materials and Structures, Xi'an Jiaotong University, Xi'an 710049, China.
E-mail address: tjlu@mail.xjtu.edu.cn (T.J. Lu).

http://dx.doi.org/10.1016/j.compscitech.2015.09.009
0266-3538/

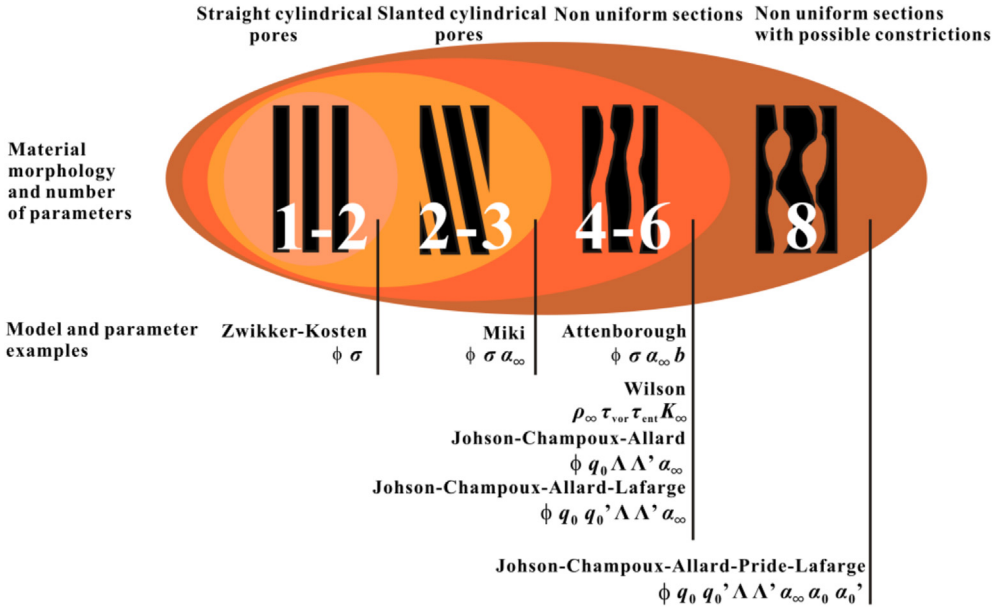

Fig. 1. Analytical models of sound absorption for porous media with rigid skeleton: complexity comparison in terms of the number of parameters needed [15].

with different cell sizes and open-pore rates and applied the scaling law [1,17] to characterize the microstructure properties with non-acoustic parameters. Focusing on the sound propagation behavior of polyurethane foams with fully/semi-open cells, Kino et al. [5,7–9] contributed essential experimental results of the non-acoustic/acoustic parameters such as tortuosity factor, Young's moduli, loss factor and flow resistivity. Besides applying the above-mentioned models including Johnson-Champoux-Allard (JCA) and Biot-Johnson-Champoux-Allard (BJCA) models to predict the SAC of polyurethane foams, they improved the prediction accuracy for JCA model by introducing a correction factor that is based upon the flow resistivity [14]. Perrot et al. [2] investigated both experimentally and numerically the non-acoustic properties of open-cell foams. Their numerical homogenization approach was based on periodic redistribution of tetrakaidecahedron unit cells, with particular focus placed upon estimating the frequency-dependent viscous-inertial and thermal responses of the foam. Also adopting the tetrakaidecahedron unit cell, Hoang and Perrot [3,18] developed a finite-element (FE) numerical homogenization approach to calculate SAC for foams with semi-open pores. It was found that the involvement of membrane in the unit cell played a vital role in viscous-inertial and thermal energy dissipation.

The studies mentioned above are all based on the tetrakaidecahedron unit cell. Although tetrakaidecahedron unit cell is thought to be a more realistic approximation to real foam topology than other types of unit cell, its complex three-dimensional (3D) structure makes it difficult to obtain purely analytical prediction of fundamental transport properties such as permeability and flow tortuosity. To predict the SAC of any porous medium, permeability is an essential parameter. Although routinely measuring the permeability (or determining via scaling law) by previous studies seems useful and convenient for SAC prediction, the physical basis and insight into this essential transport property is unclear. Further, the (viscous) permeability is as a matter of fact not an independent variable, which is an output of foam microstructure, pore size and porosity [19]. To squarely address this deficiency, this study introduces a purely analytical model of viscous permeability for foams with fully/semi-open pores as a physical basis for SAC modeling. To this end, an idealized 3D cubic unit cell with circular ligaments is employed, with thin membranes covering the pore window to represent the topological features of foams having semi-open cells. With key non-acoustic parameters deduced from the cubic unit cell, we demonstrate that the SAC of such idealized foams can be simply yet analytically predicted as a function of morphological parameters.

2. Analytical model development

2.1. Approximation of foam microstructure

To determine the transport properties of open-cell foams, a proper selection of the representative UC is essential [19,20]. Applying relevant governing equations to the selected UC, one can determine transport properties such as effective thermal conductivity, permeability, flow tortuosity and SAC. Amongst the fundamental UC models including two-dimensional (2D) hexagonal network assembling [20], cubic cell [21,22] and tetrakaidecahedron [23], cubic cell has been shown to be capable of capturing the flow characteristics in open-cell foams [19–22]. In the present study, we characterized nine foams into two groups: S3, S4, S5 and S9 with fully-open cells and S1, S2, S6, S7 and S8 with semi-open cells (see Fig. 2). For the two types of foams, corresponding UCs is built (see Fig. 3). As shown in Fig. 3(a), a cubic UC consisting of twelve ligaments (identical length a and diameter r) with a spherical node (diameter is R) at the joint is employed as the topological basis for modeling sound transport in foams with fully-open cells. For foams with semi-open cells, a modified cubic UC is developed where the window of each face is covered by a thin membrane with a circular window of diameter d_p; see Fig. 3(b). It is worth noting here that the membrane is assumed to be sufficiently thin to neglect its weight when calculating the foam porosity.

2.2. Non-acoustic properties of foams with fully-open cells

2.2.1. Viscous permeability (static flow resistance)

Based on geometrical pore-scale volumetric averaging of highly porous isotropic foams, Du Plessis et al. [21,22] proposed an analytical expression between the volume-averaged pressure gradient of fluid flow through a cubic unit cell (mimicking open-cell foams) and the corresponding viscous shear factor, expressed as:

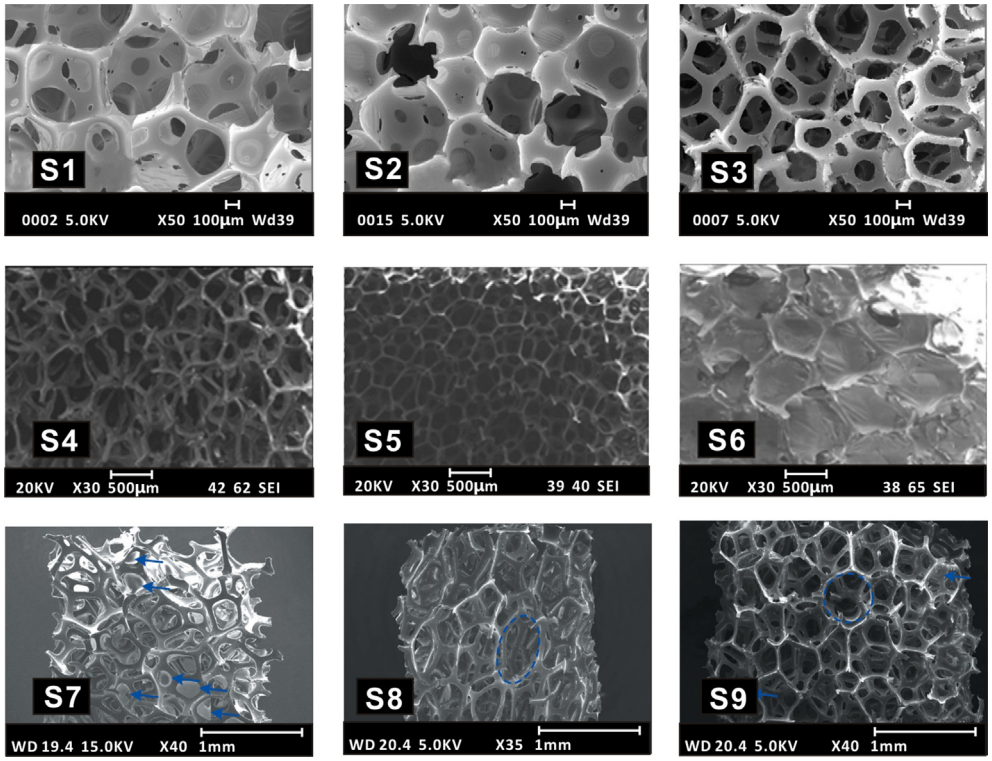

Fig. 2. Foams with fully-/semi-open pores characterized in the present study [5,6,18].

$$\nabla\langle p\rangle_f = \frac{\mu\langle v\rangle_f}{\phi} f \tag{1}$$

where $\langle p\rangle_f$ and $\langle v\rangle_f$ are the volume-averaged pressure and velocity, ϕ is the foam porosity, f is the viscous shear factor. For the low Reynolds number range, namely the Darcy flow regime, the viscous shear factor can be approximated as the drag force (f_v) in a UC (see Fig. 3) with a frontal area a^2 and a depth a [21,22]:

$$f_v = -\phi\nabla\frac{\langle p\rangle_f}{\phi}a^3 \tag{2}$$

As suggested by White [24], the drag force can be written as a function of friction coefficient, expressed as:

$$f_v = \frac{C_{D,v}\rho_f v_p^2 A_{sf}}{2} \tag{3}$$

where $C_{D,v}$ is the friction coefficient, ρ_f is the fluid density, A_{sf} denotes the wetted surface area of the cubic UC in Fig. 3(a), v_p is the average pore velocity in a longitudinally oriented pore. The volumetric flow rate through the present UC with a cross-section area A_p can be separately calculated as $v_p A_p$ and $\langle v\rangle_f a^2$. Hence, the average pore velocity v_p takes:

$$v_p = \langle v\rangle_f \frac{\chi}{\phi} \tag{4}$$

where χ is the tortuosity of fluid flow across the porous solid matrix (namely flow tortuosity but not the acoustic parameter "tortuosity

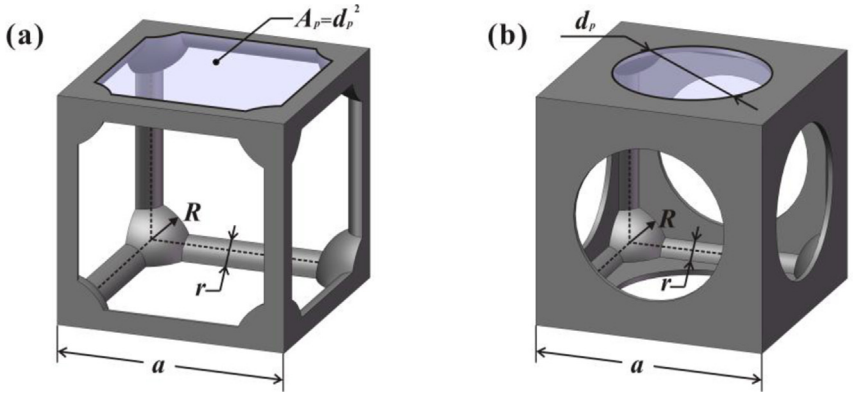

Fig. 3. Open-cell foam modeled with a cubic unit cell: (a) without membrane; (b) with membrane. a is cell size or so-called pore size, d_p is the window size, r/R is the diameter ratio of ligament to node.

factor" denoted in Section 2.2.3) and denoted as $\chi = \phi a^2/A_p$. For the friction coefficient, Du Plessis et al. [21,22] suggested that the hydrodynamic stresses at the solid–fluid interface of the UC complied to the plane Poiseuille flow at a mean pore velocity. The friction coefficient can be therefore expressed as:

$$C_{D,v} = \frac{12\mu\phi}{\rho_f v_p d_p} \tag{5}$$

where d_p is the equivalent diameter of the UC window and it is defined as $d_p^2 = A_p$.

Combining Eqs. (1)–(5) and Darcy's law for the pressure drop in a volume-averaged form, the viscous permeability (q_0) can be therefore analytically predicted as:

$$\frac{q_0}{a^2} = \frac{\phi^2 d_p a}{6\chi A_{sf}} \tag{6}$$

where the foam porosity ϕ and pore size a can be obtained from the manufacturer, the flow tortuosity χ, the equivalent diameter d_p and the wetted surface area A_{sf} can be calculated according to the topological characteristics of the cubic unit cell.

The model of Du Plessis et al. gives correct trend for viscous permeability as a function of foam porosity and their model may be used for engineering applications of flow control and pressure drop design. Although there exists discrepancy between their model prediction and experimental results (they do not consider the node size effect in their model development), they proposed an effective approach to solve volume-averaged Navier–Stokes equations within the Darcy flow regime. In what follows, we extend their model to a better predicting accuracy, favoring a good agreement with experimental measurements [20], see Fig. 4.

2.2.2. Thermal characteristic length

The thermal characteristic length characterizes the high-frequency behavior of the bulk modulus, defined as twice the average ratio of cell volume V to wetted surface A_{sf}:

$$\frac{2}{\Lambda'} = \frac{\int_A \mathrm{d}A}{\int_V \mathrm{d}V} = \frac{A_{sf}}{V} \tag{7}$$

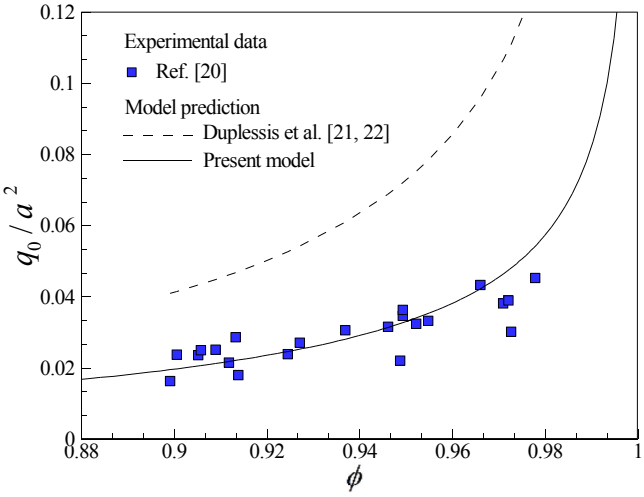

Fig. 4. Dimensionless viscous permeability as a function of foam porosity: model comparisons ($r/R = 0.6$ is thought for foams within the porosity range of 0.88–0.98).

For the unit cell depicted in Fig. 3(a) for open-cell foams, the wetted surface area can be calculated as:

$$\begin{aligned} A_{sf} =& \left(3a - 3\cdot\left(2\sqrt{R^2 - r^2}\right)\right)\cdot 2r\pi + 4R^2\pi \\ & - 12\pi R\left(R - \sqrt{R^2 - r^2}\right) + 24ar - 24r^2 \\ & + 24\left(\frac{1}{2}R^2\theta - \left(\sqrt{R^2 - r^2} - r\right)r\right) \end{aligned} \tag{8}$$

where R and r are the radius of the spherical node and circular ligament in respective, θ is defined as $\theta = \pi/2 - 2\,arcsin(r/R)$. With the UC volume calculated as a^3, the thermal characteristic length can be obtained by Eqs. (7) and (8).

2.2.3. Tortuosity factor, viscous characteristic length and thermal permeability

Tortuosity factor, denoted as α_∞, is an intrinsic property of the porous frame that is dependent upon the pore-level topology of porous materials. For porous materials having idealized topologies, the tortuosity factor may be predicted fully analytically or semi analytically [16]. In reality, however, the complex topology of open-cell foams deteriorates the possibility of analytically determining the tortuosity factor. In the present study, for simplicity, we apply the arithmetic mean (experimentally measured to be 1.05 by Doutres et al. [6]) as the value of tortuosity factor for foams having fully-open cells.

For porous materials having general topologies, the viscous characteristic length Λ is defined as [12]:

$$\frac{2}{\Lambda} = \frac{\int_A v_i^2(r_w)\mathrm{d}A}{\int_V v_i^2(r)\mathrm{d}V} \tag{9}$$

where $v_i(r_w)$ and $v_i(r)$ are separately the fluid velocity on the pore surface and inside the pore; the integral in the numerator is performed over the pore surfaces A in the representative elementary volume and the integral in the denominator is performed over the volume V of the pore.

The above definition of viscous characteristic length requires the calculation of velocity field inside a pore, which is inconvenient for SAC modeling. Johnson et al. [12] proposed a simple analytical form for Λ, as:

$$\Lambda = \frac{1}{\xi}\sqrt{\frac{8\eta\alpha_\infty}{\sigma\phi}} \tag{10}$$

where ξ is the pore shape factor and cannot be determined analytically for complex geometries. For open-cell foams, the pore shape factor obtained by Doutres et al. [6] ranges from 1.1 to 1.2 in the porosity range of 0.965–0.995. Therefore, in the present study, we average the pore shape factors as 1.146.

The thermal permeability q_0' is a complex parameter that relates the pressure time derivative to the mean temperature. Champoux and Allard [13] proposed a simple yet accurate expression relating thermal permeability to porosity ϕ and thermal characteristic length Λ', as:

$$q_0' = \frac{1}{8}\phi\Lambda'^2 \tag{11}$$

This expression is adopted in the present study.

Hitherto, the five dominant parameters (viscous/thermal permeability, viscous/thermal characteristic length, and tortuosity

factor) required to predict the SAC of open-cell foams have been analytically determined. In practice, as a result, only morphological parameters – porosity ϕ and window size d_p – need to be measured to determine the SAC, which significantly reduces the complexity and workload of SAC modeling compared with previous studies. Compared with other UC models e.g. models using scaling law or fitting correlation to determine viscous permeability [1,6,17], the analytical determination of viscous permeability paves better physical basis.

2.3. Non-acoustic properties of foams having semi-open cells

For foams with semi-open cells as depicted in Fig. 3(b), the membrane covering on the window significantly affects the five dominating parameters. As a result, the analytical models developed in the previous section for foams having fully-open cells may not give good predictions for foams having semi-open cells. Consequently, the open-pore rate, defined as the window area ratio with membrane to that without, is introduced here to modify and extend these analytical models.

2.3.1. Viscous permeability (static flow resistance)

The membrane covering on the pore window will not change the skeleton of the foam but dramatically influence the flow tortuosity and hence the static flow resistance. We employ a modified cubic unit cell as shown in Fig. 3(b) to mimic the topology of foams with semi-open cells, for which the open-pore rate R_w is calculated as:

$$R_w = \frac{\pi}{4}\left(\frac{d_p}{a}\right)^2 \tag{12}$$

Mathematical manipulation of Eq. (12) in terms of the relationship among flow tortuosity χ, the equivalent diameter d_p and the cubic cell size a ($\chi = \phi a^2/d_p^2$) leads to the flow tortuosity for foams with semi-open cells, expressed as:

$$\chi = \frac{\pi}{4}\left(\frac{\phi}{R_w}\right) \tag{13}$$

Finally, by combining Eqs. (6), (8) and (13), the static flow resistance of foams with semi-open cells can be analytically predicted as a function of foam porosity, window size, and open-pore rate.

2.3.2. Thermal characteristic length

The definition of thermal characteristic length requires determining the specific surface area of a representative UC. For foams with semi-open cells, it takes the following form:

$$\Lambda' = \frac{2V}{A_s + (1 - R_w)A_p} \tag{14}$$

where A_s is the surface area of cell ligaments inside a representative UC of volume V and can be calculated by analyzing the geometric features as:

$$A_s = \left(3a - 3\cdot\left(2\sqrt{R^2 - r^2}\right)\right)\cdot 2r\pi + 4R^2\pi - 12\pi R\left(R - \sqrt{R^2 - r^2}\right) \tag{15}$$

With the pore surface area (window size A_p) and cell volume (V) separately calculated by $A_p = \pi d_p^2/4$ and $V = a^3$, the thermal characteristic length can be analytically predicted through substituting Eq. (15) into Eq. (14).

2.3.3. Tortuosity factor, viscous characteristic length and thermal permeability

For fully-open foams, we employ the arithmetic mean value (1.05 as measured by Doutres et al. [6]) to represent the tortuosity factor α_∞. Increasing the open-pore rate dramatically increases the tortuosity factor. Following Doutres et al. [6], an empirical correlation is used for various kinds of semi-open foams, expressed as:

$$\alpha_{\infty\text{semi}}/\alpha_\infty \sim R_w^n \tag{16}$$

where $\alpha_{\infty\text{semi}}$ is the tortuosity factor for semi-open foams and n is the correlating index.

To calculate the viscous characteristic length, Eq. (10) is continuously used but the pore shape factor (ξ) needs to be correlated with the open-pore rate (R_w) in order to represent the pore shape of semi-open foams. Similar to Eq. (16), we propose:

$$\xi_{\text{semi}}/\xi \sim R_w^t \tag{17}$$

where ξ_{semi} is the pore shape factor for semi-open foams and t is the correlating index.

As for the thermal permeability, Eq. (11) can be used when the thermal characteristic length is determined by Eq. (14).

2.4. Sound absorption coefficient: John-Champoux-Allard model

To determine the SAC of a porous medium, determinations of the effective density ρ_{eq} and bulk modulus K_{eq} of the saturating fluid are essential. Once ρ_{eq} and K_{eq} are known, the SAC (denoted as α_{SAC}) for a porous medium can be obtained by:

$$\alpha_{SAC} = \frac{4\rho_0 c\,\mathrm{Re}\left(\sqrt{\rho_{eq}K_{eq}}\coth\left(j\omega L\sqrt{\rho_{eq}/K_{eq}}\right)\right)}{\left(\mathrm{Re}\left(\sqrt{\rho_{eq}K_{eq}}\coth\left(j\omega L\sqrt{\rho_{eq}/K_{eq}}\right)\right) + \rho_0 c\right)^2 + \mathrm{Im}\left(\sqrt{\rho_{eq}K_{eq}}\coth\left(j\omega L\sqrt{\rho_{eq}/K_{eq}}\right)\right)^2} \tag{18}$$

where Re and Im refer to the function of real and imaginary part of a parameter, ρ_0 is the density of the saturating fluid without acoustical stimulation at ambient temperature and pressure, j is imaginary unit, ω is the sound angular frequency, and c is the sound speed at ambient temperature and pressure.

Numerous efforts have been devoted to analytically determining ρ_{eq} and K_{eq} of the fluid saturated in a given porous medium. Among these analytical models, the Johnson-Champoux-Allard (JCA) model is capable of giving satisfactory SAC prediction yet requiring relatively less parameters [16]. The effective density of the fluid saturating a porous frame is obtained by Johnson et al. [11] as:

$$\rho_{eq} = \frac{\rho_0}{\phi}\left[\alpha_\infty + \frac{\nu\phi}{j\omega q_0}\sqrt{1+\left(\frac{2\alpha_\infty q_0}{\phi\Lambda}\right)^2 \frac{j\omega}{\nu}}\right] \tag{19}$$

while the bulk modulus of the fluid is predicted by Champoux and Allard [13] as:

$$K_{eq} = \frac{\gamma P_0}{\phi}\left(\gamma - \frac{\gamma-1}{1+\frac{\nu'\phi}{j\omega q_0'}\sqrt{1+\left(\frac{\Lambda'}{4}\right)^2 \frac{j\omega}{\nu'}}}\right)^{-1} \tag{20}$$

Thus, the JCA model requires five parameters to determine the SAC of open-cell foams: foam porosity ϕ, tortuosity factor α_∞, flow permeability q_0, viscous characteristic length Λ and thermal characteristic length Λ'. Other relevant parameters including the kinematic viscosity ν, thermal diffusivity ν' and specific heat capacity γ of the fluid are given by the values obtained under atmospheric pressure P_0 and temperature T_0.

3. Discussion of results

3.1. Validation of analytical prediction for non-acoustic properties

Fig. 2 depicts the nine polyurethane foam samples with fully- or semi-open pores that are characterized in the present study using existing non-acoustic and SAC measurement data: samples S1, S2 and S3 are taken from Kino et al. [5], S4, S5 and S6 from Doutres et al. [6]; S7, S8 and S9 from Hoang et al. [18]. Basic morphological parameters of these foam samples are listed in Table 1. It is seen from Fig. 2 that the skeleton of foams with semi-open cells (S1, S2, S6, S7 and S8) is the same as that of foams with fully-open cells (S3, S4, S5 and S9), favoring the assumptions made in unit cell construction (Fig. 3).

The model predictions of viscous/thermal characteristic length and viscous permeability are compared with existing experimental results. Overall, satisfactory agreement is achieved, validating the present analytical model. The viscous/thermal characteristic length and viscous permeability of semi-open foams are much lower than those of fully-open foams, which is attributed mainly to the presence of thin membrane covering on pore window. For instance, the thermal characteristic length of foam S1 is less than 10% of that of foam S3 having the same porosity (see Table 1). Detailed comparisons among different non-acoustic parameters are presented in Table 1, as well.

The influence of membrane upon the three dominating non-acoustic parameters is qualitatively analyzed as follows: (1) as viscous characteristic length accounts for the average pore window diameter, the smaller the pore window diameter is, the shorter the viscous characteristic length is; (2) as thermal characteristic length both qualitatively and quantitatively reveals the specific area, significant increase in specific area caused by the membrane leads to significant reduction in thermal characteristic length; (3) as viscous permeability accounts for the viscous flow resistance, the smaller the window diameter is, the lower the viscous permeability (the higher the flow resistance) is.

Viscous permeability (static flow resistance) is usually determined by direct measurement or scaling law: purely analytical modeling of viscous permeability attracts little attention. Doutres et al. [6] applied the scaling law proposed by Lind-Nordgren and Göransson [1,17] to predict the static flow resistance of fully-open foams and achieved good agreement with experimental results. However, the scaling law requires several implicit assumptions without clear physical meaning including cylindrical pore ($\xi = 1$), $\phi \approx 1$ and $\alpha_\infty \approx 1$. Doutres et al. [6] admitted that their satisfactory prediction of static flow resistance surprised them, as well.

For viscous and thermal characteristic lengths, the correlation $\Lambda'/\Lambda = 2$ suggested by Allard and Atalla [16] is sometimes used to determine the other one once one of the characteristic lengths is

Table 1
Comparison of non-acoustic parameters for foams obtained from experiments (S1, S2 and S3 are from Ref. [5]; S4, S5 …, S9 are from Ref. [6]), numerical simulation [18] and the present model prediction.

No.	d_p/μm	Source	ϕ	Λ'/μm	$q_0 \times 10^{-9}$/m^2	Λ/μm	α_∞	q_0' $\times 10^{-9}$/m^2
S1	498	Experiment	0.978	47	0.124	23	1.111	/
		Simulation	0.98	156 ± 42	0.124	39 ± 4	2.856 ± 0.551	3.74 ± 2.14
		Model	0.978	75	0.331	17.76	2.8559	0.688
S2	535	Experiment	0.946	70	0.242	35.1	1.1592	/
		Simulation	0.945	168 ± 24	0.242	53 ± 4	2.333 ± 0.246	4.23 ± 1.18
		Model	0.946	77	0.461	25.8	2.33328	0.716
S3	622	Experiment	0.978	482	5.81	161	1.0584	/
		Simulation	0.98	482 ± 175	5.81	277 ± 111	1.050 ± 0.053	13.38 ± 2.84
		Model	0.978	580	9.77	248.82	1.05	41.15
S4	574	Experiment	0.987 ± 0.01	435 ± 38	10.97 ± 0.79	269 ± 6	1.042 ± 0.006	/
		Simulation	0.97 ± 0.02	641 ± 314	5.84 ± 3.99	366 ± 181	1.026 ± 0.015	11.53 ± 7.51
		Model	0.987	557.6	10.37	256.11	1.05	38.087
S5	453	Experiment	0.968 ± 0.01	268 ± 16	4.94 ± 0.16	183 ± 1	1.059 ± 0.001	/
		Simulation	0.94 ± 0.02	398 ± 119	2.94 ± 1.29	228 ± 68	1.043 ± 0.02	6.02 ± 2.47
		Model	0.968	324.34	4.39	168.5	1.05	12.62
S6	987	Experiment	0.977 ± 0.01	286 ± 30	1.62 ± 0.16	59 ± 12	2.301 ± 0.092	/
		Simulation	0.98 ± 0.02	336 ± 8	1.62	96 ± 7	1.907 ± 0.118	16.3 ± 0.92
		Model	0.977	154.02	2.17	53.70	2.396	2.89
S7	585	Experiment	0.98 ± 0.01	/	2.60 ± 0.08	/	/	/
		Simulation	0.98	288 ± 4	/	138 ± 7	1.17 ± 0.02	8.56 ± 0.10
		Model	0.98	194.39	3.20	119.35	1.15	4.63
S8	648	Experiment	0.97 ± 0.01	/	2.98 ± 0.14	/	/	/
		Simulation	0.97	308 ± 7	/	147 ± 6	1.18 ± 0.02	10.04 ± 0.23
		Model	0.97	175.76	2.74	105.03	1.18	3.75
S9	503	Experiment	0.98 ± 0.01	/	4.24 ± 0.29	/	/	/
		Simulation	0.98	438 ± 25	/	261 ± 19	1.04 ± 0.01	9.27 ± 0.67
		Model	0.98	488.63	6.65	205.14	1.05	29.25

Note: the thicknesses of S1, S2 and S3 are separately 20.3 mm, 20.4 mm and 20.0 mm; the thicknesses of S4, S5 and S6 are all 49 mm; and the thicknesses of S7, S8 and S9 are separately 25 mm, 15 mm and 15 mm.

determined. However, this ratio (Λ'/Λ) may have different values for different kinds of foams, e.g., $\Lambda'/\Lambda = 1.55$ as correlated by Doutres et al. [6]. Therefore, to better understand the physical basis of and provide further insight into foam transport properties, analytical models that can separately predict viscous and thermal characteristic lengths are preferred.

3.2. Validation of analytical prediction for sound absorption coefficient

Analytical predictions, numerical computations and experimental measurements [3,5,6] of the SAC are compared in Fig. 5 for the 9 foam samples (rigid backing) listed in Table 1. The present analytical model is seen to be capable of capturing the variation trend of SAC in the frequency range of 0–4500 Hz, showing satisfactory agreement with experimental data. The underestimated SAC in Fig. 5 (d), (e), (g) and (h) is mainly due to the lacking of information for bulk modulus (K_{eq}) in the JCA model [11,13] we applied. Only two parameters, porosity ϕ and thermal characteristic length Λ', are involved in the JCA model to account for the thermal effect during sound propagation in porous materials. More sophisticated models such as the Johnson-Champoux-Allard-Lafarge (JCAL) model [11,13,25] or the Johnson-Champoux-Allard-Pride-Lafarge (JCAPL) model [11,13,25,26] can give better predictions especially in the low frequency range. However, the JCAL and JCAPL models require more non-acoustic parameters to be determined, and some cannot be analytically determined or readily measured. Hence, for foams with fully- or semi-open cells, the JCA model is capable of giving sufficiently prediction accuracy.

The nine polyurethane foams may be categorized into two groups: (1) S3, S8 and S9 which do not exhibit SAC peaks; (2) S1, S2, S4, S5, S6 and S7 which exhibit SAC peaks. The absence of SAC peak in Group (1) is because the 1/4 Wavelength Resonance Frequencies (1/4 WRFs) of foam S3, S8 and S9 are a little bit higher than the frequency range considered in the present study. For Group (2), the existence of SAC peak for foam S2, S4, S5, S6 and S7 is due mainly to their relatively small 1/4 WRF. For foam S6, SAC peaks and valleys at 1/4, 2/4 and 3/4 WRF are observed in Fig. 5(f). Particularly, in Fig. 5(a), the experimentally measured SAC for S1 dramatically jumps near 1200 Hz, which is neither captured by the present analytical model nor by numerical simulation [18]. It is believed that such a jump in SAC is caused by the local resonances of an elastic solid skeleton, which the present JCA model as well as the numerical simulation does not take into account. To justify the effect of Young's modulus on the sound transmit in elastic foams, Kino's research group [5,7–9] did a series of investigations and gave plenty of discussions on this issue experimentally, numerically and theoretically.

In summary, the results of the present study suggest that the cubic UC is capable of capturing both the flow and microstructure characteristics of foams having either fully-open or semi-open cells, successfully establishing a link between SAC and foam topologies. The purely analytical models for viscous permeability and thermal characteristic length reduce the experimental workload for key non-acoustic parameters and increase the model robustness. For fully-open foams, satisfactory SAC prediction relative to experimental measurement is obtained by using only two morphological parameters (porosity ϕ and pore window size d_p) as input information. For semi-open foams, similarly good agreement between SAC prediction and measurement is achieved by introducing an additional parameter (open-pore rate R_w) into the model.

4. Conclusions

This study presents an analytical model that can predict sound absorption coefficient (SAC) in open-cell foams. Compared with the

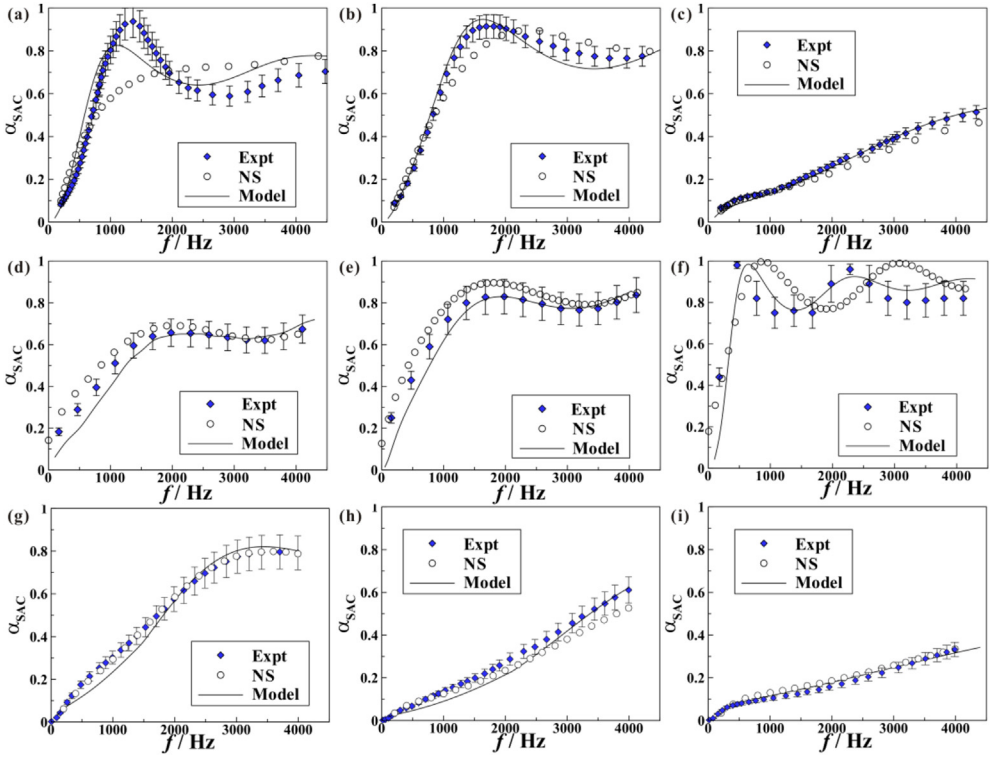

Fig. 5. Sound absorption coefficient plotted as a function of frequency for foams having fully-open or semi-open cells: (a) S1; (b) S2; (c) S3; (d) S4; (e) S5; (f) S6; (g) S7; (h) S8; (i) S9. Note: "Expt" refers to experimental results taken from Refs. [3,5,6]; "NS" refers to numerical simulation results [3,5,6,18]; "Model" refers to the present analytical model prediction.

experimental and numerical results, the present model gives satisfactory agreement on SAC prediction. The results demonstrate that: i) the idealized cubic unit cell is capable of representing foam topology on sound propagation; ii) as viscous permeability (stagnant flow resistance) serving the predomination, Johson-Chmpoux-Allard model can accurately describe the sound propagation in porous materials with rigid body; iii) to predict SAC of rigid foams, porosity and pore window size are the governing parameters for fully open cells; open-pore rate should be considered for foams with semi open cells, as well.

Acknowledgment

This work was supported by the National Natural Science Foundation of China (51506160), National 111 Project of China (B06024), the National Basic Research Program of China (2011CB610305), and the Beijing Key Lab of Heating, Gas Supply, Ventilating and Air Conditioning Engineering (NR2015K01 & NR2016K01).

References

[1] E. Lind-Nordgren, P. Göransson, Optimising open porous foam for acoustical and vibrational performance, J. Sound. Vib. 329 (7) (2010) 753–767.
[2] C. Perrot, F. Chevillotte, M.T. Hoang, G. Bonnet, F.X. Bécot, L. Gautron, A. Duval, Microstructure, transport, and acoustic properties of open-cell foam samples: experiments and three-dimensional numerical simulations, J. Appl. Phys. 111 (1) (2012) 014911–014916.
[3] M.T. Hoang, C. Perrot, Solid films and transports in cellular foams, J. Appl. Phys. 112 (5) (2012) 054911–054916.
[4] C. Perrot, R. Panneton, X. Olny, Periodic unit cell reconstruction of porous media: application to open-cell aluminum foams, J. Appl. Phys. 101 (11) (2007) 113538–113610.
[5] N. Kino, G. Nakano, Y. Suzuki, Non-acoustical and acoustical properties of reticulated and partially reticulated polyurethane foams, Appl. Acoust. 73 (2) (2012) 95–108.
[6] O. Doutres, N. Atalla, K. Dong, Effect of the microstructure closed pore content on the acoustic behavior of polyurethane foams, J. Appl. Phys. 110 (6) (2011) 064901–064911.
[7] N. Kino, T. Ueno, Experimental determination of the micro-and macrostructural parameters influencing the acoustical performance of fibrous media, Appl. Acoust. 68 (11) (2007) 1439–1458.
[8] N. Kino, T. Ueno, Evaluation of acoustical and non-acoustical properties of sound absorbing materials made of polyester fibres of various cross-sectional shapes, Appl. Acoust. 69 (7) (2008) 575–582.
[9] N. Kino, T. Ueno, Comparisons between characteristic lengths and fibre equivalent diameters in glass fibre and melamine foam materials of similar flow resistivity, Appl. Acoust. 69 (4) (2008) 325–331.
[10] M.A. Biot, Theory of propagation of elastic waves in a fluid-saturated porous solid. II. Higher frequency range, J. Acoust. Soc. Am. 28 (2) (1956) 179–191.
[11] D.L. Johnson, J. Koplik, R. Dashen, Theory of dynamic permeability and tortuosity in fluid-saturated porous media, J. Fluid Mech. 176 (3) (1987) 379–402.
[12] D.L. Johnson, J. Koplik, L.M. Schwartz, New pore-size parameter characterizing transport in porous media, Phys. Rev. Lett. 57 (20) (1986) 2564–2567.
[13] Y. Champoux, J.F. Allard, Dynamic tortuosity and bulk modulus in air-saturated porous media, J. Appl. Phys. 70 (4) (1991) 1975–1979.
[14] N. Kino, T. Ueno, Improvements to the Johnson–Allard model for rigid-framed fibrous materials, Appl. Acoust. 8 (11) (2007) 1468–1484.
[15] http://apmr.matelys.com/index.html.
[16] J.F. Allard, N. Atalla, Propagation of Sound in Porous Media: Modelling Sound Absorbing Materials, second ed., John Wiley & Sons, New York, 2009, p. 84.
[17] P. Göransson, Acoustic and vibrational damping in porous solids, Philos. Trans. R. Soc. A 364 (1838) (2006) 89–108.
[18] M.T. Hoang, C. Perrot, Identifying local characteristic lengths governing sound wave properties in solid foams, J. Appl. Phys. 113 (8) (2013) 084905–084907.
[19] X.H. Yang, T.J. Lu, T. Kim, An analytical model for permeability of isotropic porous media, Phys. Lett. A 378 (30) (2014) 2308–2311.
[20] A. Bhattacharya, Thermophysical Properties and Convective Transport in Metal Foams and Finned Metal Foam Heat Sinks, D Phil, University of Colorado, 2002.
[21] P. Du Plessis, A. Montillet, J. Comiti, J. Legrand, Pressure drop prediction for flow through high porosity metallic foams, Chem. Eng. Sci. 49 (21) (1994) 3545–3553.
[22] J.G. Fourie, J.P. Du Plessis, Pressure drop modelling in cellular metallic foams, Chem. Eng. Sci. 57 (14) (2002) 2781–2789.
[23] X.H. Yang, J.J. Kuang, T.J. Lu, F.S. Han, T. Kim, A simplistic analytical unit cell based model for the effective thermal conductivity of high porosity open-cell metal foams, J. Phys. D. Appl. Phys. 46 (25) (2013) 255302–255306.
[24] F.M. White, I. Corfield, Viscous Fluid Flow, third ed., McGraw-Hill, New York, 2006.
[25] D. Lafarge, P. Lemarinier, J.F. Allard, V. Tarnow, Dynamic compressibility of air in porous structures at audible frequencies, J. Acous Soc. Am. 102 (4) (1997) 1995–2006.
[26] S.R. Pride, F.D. Morgan, A.F. Gangi, Drag forces of porous-medium acoustics, Phys. Rev. B 47 (9) (1993) 4964–4979.